Function-Based Modulation Control for Modular Multilevel Converters under Varying Loading and Parameters Conditions

Majid Mehrasa [1], Edris Pouresmaeil [2,3], Mudathir Funsho Akorede [4], Sasan Zabihi [5], and João P. S. Catalão [2,3,6,*]

[1] Young Researchers and Elite Club, Sari Branch, Islamic Azad University, Sari, Iran
[2] INESC-ID, Inst. Super. Tecn., University of Lisbon, Av. Rovisco Pais, 1, 1049-001 Lisbon, Portugal
[3] C-MAST, University of Beira Interior, R. Fonte do Lameiro, 6201-001 Covilhã, Portugal
[4] Department of Electrical & Electronics Engineering, University of Ilorin, 240003 Ilorin, Nigeria.
[5] ABB Australia, MicroGrid, Renewable Integration and Distributed Generation CoC, 3406 Export Drive, Berrimah, Northern Territory 0828, Australia
[6] INESC TEC and Faculty of Engineering of the University of Porto, R. Dr. Roberto Frias, 4200-465 Porto, Portugal

[*]correspondence: catalao@fe.up.pt

Abstract: This paper presents a new function-based modulation control technique for modular multilevel converters (MMC). The main contribution of the study is the formulation of two new modulation functions for the required switching signals of the MMC's upper and lower sub-modules respectively. The output and circulating current equations of the converter are employed to attain the arm's currents which are utilized for the proposed modulation functions, which have two important features: i) it is much less complex compared to the existing control methods of MMC; and ii) the proposed controller can be regulated properly to deal with parameter variations in a bid to ensure stable and accurate performance. In this controller, the MMC output current magnitude and phase angle required for special active and reactive power sharing can be easily applied to the modulation functions. Also, the equivalent capacitors of upper and lower sub-modules are discussed based on the proposed modulation functions. Finally, simulations are performed in Matlab/Simulink environment to evaluate the performance of the proposed control technique in both the dynamic conditions of load as well as varying parameters.

Keywords: Modular Multilevel Converter, Modulation Function, Control, Parameters Variations, Sub-Modules.

1. Nomenclature

Indices		α	Angle Difference between output MMC voltages and Currents
k	a,b,c	Θ_i	Phase angle of modulation functions
j	0,-1,1	***Parameters***	
i	u,l	L	Output inductance of MMC
Abbreviation		R	Output resistance of MMC

MMC	Modular Multilevel Converter	L_t	Arm's inductance of MMC
SLPWM	Shift Level Pulse Width Modulation	R_t	Arm's resistance of MMC
Variables		L_{eq}	Equivalent inductance of MMC
i_k	Input MMC Currents	R_{eq}	Equivalent resistance of MMC
i_{lk}	Arm Currents of MMC	ω	Angular frequency of MMC
i_{cirk}	Circulating Currents of MMC	$\beta_{i(012)}$	Harmonically coefficients of sub-module powers
i_{dc}	MMC dc-link Current	$\beta_{xi(012)}$	Harmonically coefficients of arm's inductance and resistance powers
v_{dc}	MMC dc-link Voltage	$q_{3\varphi}$	Output Reactive power of MMC
v_{ik}	Sub-modules Voltages of MMC	I_{dc}	dc component of dc-link current
v_k	Output voltages of MMC	$\boldsymbol{i}_{dcrip}$	Ripple parts of dc-link current
v_{ix}	The voltage of arm's resistance and inductance	$\tilde{i}_{dcrip}$	Derivative of dc-link current ripple parts
p_{ik}	Sub-modules power of MMC	I_m	Magnitude of output MMC Currents
p_{ix}	The power of arm's resistance and inductance	V_m	Maximum Magnitude of output MMC Voltages
$p_{3\varphi}$	Output Active power of MMC	V_{mi}	Magnitude of the proposed modulation functions

2. Introduction

Various characteristics of modular multilevel converters (MMCs) in high-power and medium-voltage applications lead to the essential need to design appropriate controllers [1-2] and proposing effective modulation techniques [3-4] for these kinds of converters. One of the significant trends for controlling the MMC is to present a dynamic model based on the considered state variables of the controller. For example, in [5], the sum of the capacitor voltage in each arm is used instead of the individual capacitor voltages to shape the MMC model. To complete the MMC evaluation, an effective dc-bus model from the sub-module capacitors is derived in [5]. For a grid-connected MMC, a natural charge level mechanism for branch capacitor voltages as well as the branch power equations based on the consumed active and reactive power in the respective resistance and inductance are investigated in [6]. The study, in addition to enhancement of the voltage ripple estimation concept using accurate model, two independent explicit control loops have also been designed for the line and circulating currents in a decoupled manner.

Another dynamic model-based assessment for the MMC-based multi-terminal HVDC (MTDC) system is performed in [7]. Two different dynamic models are proposed in the study. The first dynamic model of MMC-MTDC system is included the AC side circuit, the inner controllers, the modulation strategies, the outer controllers and the MTDC circuit. The second one as a simplified model contains the outer controllers and partial dynamics of the MTDC circuit based on a quantitative analysis of the detailed model's dynamic processes [7].

In addition to proposing a continuous equivalent model [8], a corresponding single-phase circuit and a load model consisting of current sources [9], and a dynamic model with four independent dynamical components of the arm currents with the effect of AC and DC systems [10]. Others include a discrete-time mathematical model with a predictive model [11], a linearized analytical models with droop control [12] for MMCs under balanced conditions, and other literatures that present more dynamic models and respective controllers for assessment of the MMC operation under other operating conditions [13-15].

Similarly, a number of new pulse-width modulation (PWM) techniques and capacitor voltage balancing methods have been proposed to control MMCs in different industrial applications [16-17]. A phase-disposition (PD) sinusoidal PWM strategy with a voltage balancing method [18], a voltage-balancing control method with phase shifted carrier-based PWM [19], an improved PWM method of which no phase-shifted carrier is needed [20] and a modified nearest level modulation method with the increased level number of ac output voltage [21] have been employed for MMCs. In [22], a discontinuous modulation technique based on adding a zero-sequence to the original modulation signals is proposed which can achieve a significant reduction in the capacitor voltage ripples as well as in the switching power losses for most of the operating points.

To avoid the major drawbacks of the present voltage balancing methods, such as voltage sorting algorithm, extra switching actions, interference with output voltage, the authors of [23] proposed an improved PWM based general control structure for the MMC inverters. The designed control technique is appropriate for both voltage-based and energy-based control methods, and also includes voltage balancing between the upper and lower arms [23]. With the aim of dominating the magnitude modulation for few numbers of cells and also reducing the sorting efforts for cell balancing purposes, tolerance band methods are used for MMC in [24] to obtain switching instants and also cell selection. Moreover, two different modulation patterns for multilevel selective harmonic elimination (MSHE) PWM as well as a method for selecting the number of sub-modules are proposed for control of MMC operation [25]. Among the different control and modulation methods for MMCs [26], multi-carrier PWM techniques have an effect not only on output waveforms and number of levels derived out of a given configuration of the MMC but also on DC-link voltage and arm currents of the converter [27].

In this paper, two new modulation functions are proposed for control of the MMC operation in inverter mode which can appropriately achieve the main control purposes included regulating the sub-modules voltages and executing accurate active and reactive power sharing. These modulation functions are obtained by making the circulating currents approach zero value and using the arm's currents in the basic differential equations of the MMC in a-b-c reference frame.

The main contributions of the proposed controller are: 1) achieving two separate modulation functions to attain the switching signals of upper and lower sub-modules; 2) the simplicity of the designed controller especially in comparison with the existing methods; and 3) maintaining stable operation during parameters varying condition due to its structure. Moreover, the effects of the MMC parameters and currents changes are considered as the assessment factors of the proposed modulation functions performance in both steady-state and dynamic conditions. In addition, using the proposed functions, the instantaneous powers of the MMC arms and the equivalent capacitors of the upper and lower sub-modules are evaluated. Simulation results are presented to justify the proposed modulation-based method.

3. The proposed modulation functions

The basic structure of the proposed three-phase MMC considered in the paper is shown in Fig.1.a. The dc-link voltage generates the input power needed for the MMC operation. Each arm consists of resistance and inductance, and N series-connected sub-modules, illustrated in Fig.1.b. Each sub-module acts as a voltage source which is actually a half-bridge rectifier with determined output capacitor corresponding to its required dc voltage. Based on Fig.1.b, complementary state exists for the upper and lower switches of the sub-module.

It means that if the upper switch is on, the lower switch will be off and vice versa. Moreover, the output of MMC contains inherent resistance and filter inductance. A point of common coupling (PCC) is considered in the proposed MMC in stand- alone mode as depicted in Fig.1.a, to which the output capacitance filter and the consumable three-phase load are connected. The following discusses the process of obtaining the proposed modulation function for the described MMC.

3.1. Calculation of The MMC' Arms Currents

According to Fig.1.a, supposing that MMC is controlled to reach sinusoidal output voltages at PCC and supply full three-phase load as a linear load. Thus, based on the needed active and reactive power of the load and the above conditions, the output voltage and current of MMC can be written as,

$$\begin{aligned} v_k &= v_m \cos\left(\omega t + j\frac{2\pi}{3}\right) \\ i_k &= I_m \cos\left(\omega t + j\frac{2\pi}{3} + \alpha\right) \end{aligned} \tag{1}$$

The phase angle, α is the determining variable for generating the required active and reactive power of the load in different operating conditions. From Fig.1.a, the relations between output and arm's currents of MMC and also circulating currents can be written as,

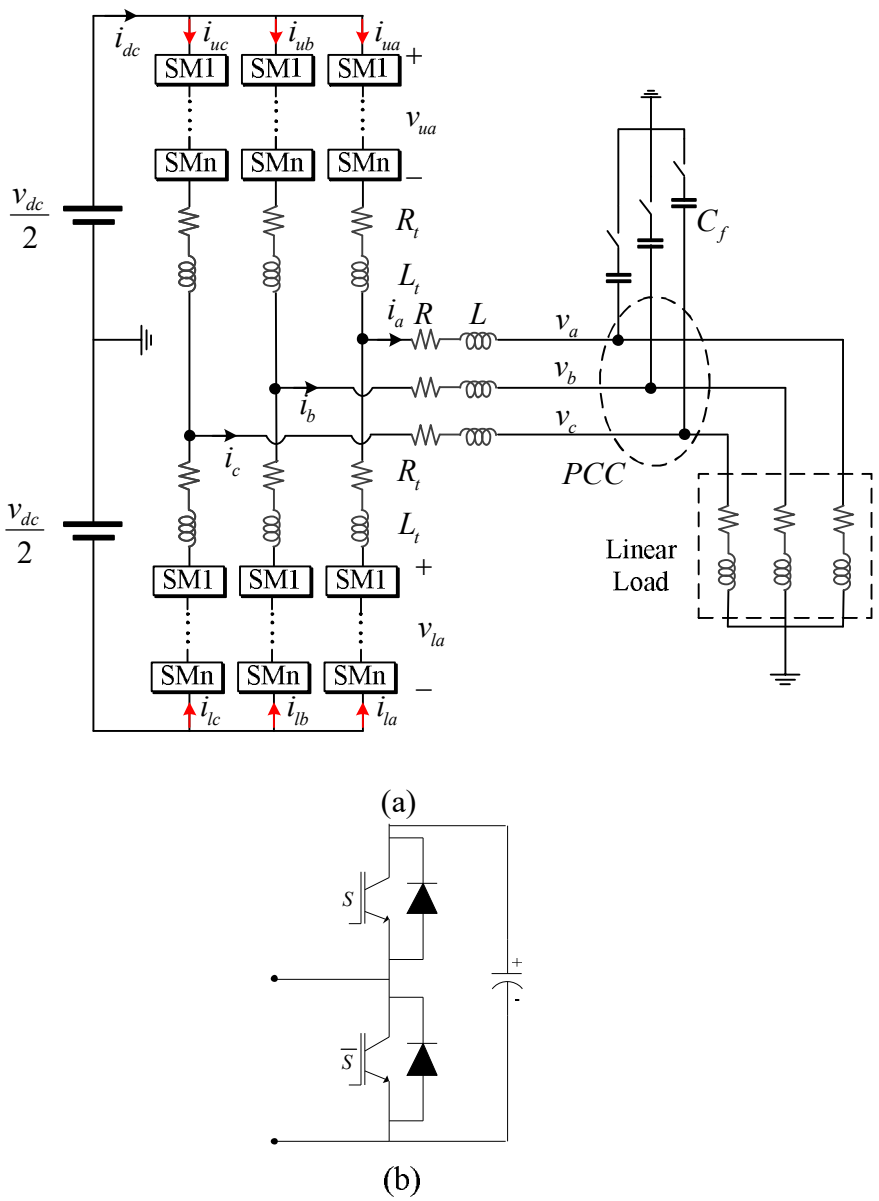

***Fig. 1**. (a) The proposed MMC, (b) sub-module.*

$$i_k = i_{uk} + i_{lk} \tag{2}$$

$$i_{cirk} = \frac{\left(i_{uk} - i_{lk}\right)}{2} - \frac{i_{dc}}{3} \tag{3}$$

For a controlled MMC with accurate operation, the circulating currents should approach zero. Consequently, by applying $i_{cirk} = 0$ to (3) and solving two equations achieved from (2) and (3), the currents of the upper and lower arms of the MMC can be written as,

$$i_{uk} = 0.5I_m \cos\left(\omega t + j\frac{2\pi}{3} + \alpha\right) + i_{dc}/3 \tag{4}$$

$$i_{lk} = 0.5I_m \cos\left(\omega t + j\frac{2\pi}{3} + \alpha\right) - i_{dc}/3 \tag{5}$$

It is understood from (4) and (5) that each arm's current is combined with the output ac and input dc currents.

3.2. The Proposed Modulation Function

For accurate control of the MMC, a well-designed pulse width modulation should be set. Therefore, two reference waveforms for upper and lower sub-modules of the MMC are proposed in this sub-section to perform a complete switching samples in the used shift-level PWM. Taking into account the neutral point of the dc link in Fig.1.a, and using KVL's law in the determined direction, equations of (6) and (7) are achieved as,

$$\frac{-v_{dc}}{2}+v_{uk}+L_t\frac{di_{uk}}{dt}+R_t i_{uk}+L\frac{di_k}{dt}+Ri_k+v_k=0 \tag{6}$$

$$\frac{v_{dc}}{2}-v_{lk}+L_t\frac{di_{lk}}{dt}+R_t i_{lk}+L\frac{di_k}{dt}+Ri_k+v_k=0 \tag{7}$$

Substituting (1) and (4) into (6) and assuming $i_{dc}=I_{dc}+i_{dcrip}, di_{dcrip}/dt=\tilde{i}_{dcrip}, L_{eq}=0.5L_t+L$ and $R_{eq}=0.5R_t+R$, the upper sub-modules voltages of the MMC can be obtained as,

$$\begin{aligned} v_{uk}=&\frac{v_{dc}}{2}-L_t\tilde{i}_{dcrip}/3-i_{dc}R_t/3+\left[I_mR_{eq}\sin(\alpha)+L_{eq}I_m\omega\cos(\alpha)\right]\sin\left(\omega t+j\frac{2\pi}{3}\right)+\\ &\left[L_{eq}I_m\omega\sin(\alpha)-I_mR_{eq}\cos(\alpha)+v_m\right]\cos\left(\omega t+j\frac{2\pi}{3}\right)\end{aligned} \tag{8}$$

Using the relation below,

$$\gamma\sin(\omega t)+\lambda\cos(\omega t)=\sqrt{\gamma^2+\lambda^2}\cos\left(\omega t+tag^{-1}(\lambda/\gamma)-\pi/2\right) \tag{9}$$

The proposed modulation function related to the switching signals of the upper sub-modules is established as (10),

$$u_{uk}=\frac{\frac{v_{dc}}{2}-L_t\tilde{i}_{dcrip}/3-i_{dc}R_t/3+V_{mu}\cos\left(\omega t+j\frac{2\pi}{3}+\theta_u-\pi/2\right)}{v_{dc}} \tag{10}$$

Please note that V_{mu} and θ_l are given in appendix A. Applying the same scenario for equation (7), the proposed modulation function for lower sub-modules is derived as (11),

$$u_{lk}=\frac{\frac{v_{dc}}{2}-L_t\tilde{i}_{dcrip}/3-R_ti_{dc}/3+V_{ml}\cos\left(\omega t+j\frac{2\pi}{3}+\theta_l-\pi/2\right)}{v_{dc}} \tag{11}$$

The variables V_{ml} and θ_l are specified in Appendix A. These functions can be used for the MMC control in all operating conditions including both dynamic and steady states. The proposed modulation functions in steady state can be achieved by substituting the reference values of the

MMC parameters and specifications in V_{mi} and θ_i as well as using the desired values of dc link voltage and current in (10) and (11).

4. Evaluation of the instantaneous power of the MMC arms

To analyze the effects of the arm's currents obtained in (4) and (5) on the MMC operation, the instantaneous power of the arms is investigated in this section. Each arm power of the proposed MMC can be included; instantaneous powers caused by sum capacitors used in the sub-modules as well as the resistance and inductance of the arms. Discussed next is the two types of power.

4.1. Instantaneous Power of the MMC sub-modules

As it can be seen in Fig.1.a, the currents of the upper arms of the MMC enter the positive point of the upper sub-modules voltage. Thus, to comply with the power's law, the instantaneous power of the MMC's upper sub-modules can be written as,

$$p_{uk} = i_{uk} v_{uk} \tag{12}$$

Substituting the obtained current and voltage corresponding to the upper sub-modules into (12), we achieve equation (13) as,

$$\begin{aligned} p_{uk} &= \left(0.5I_m \cos\left(\omega t + j\frac{2\pi}{3} + \alpha\right) + i_{dc}/3\right) \times \left(\frac{v_{dc}}{2} - L_t \tilde{i}_{dcrip}/3 - i_{dc}R_t/3 + V_{mu}\cos\left(\omega t + \theta_u - \pi/2\right)\right) \\ &= 0.25 v_{dc} I_m \cos\left(\omega t + j\frac{2\pi}{3} + \alpha\right) - \frac{I_m L_t \tilde{i}_{dcrip}}{6}\cos\left(\omega t + j\frac{2\pi}{3} + \alpha\right) - \frac{i_{dc}R_t I_m}{6}\cos\left(\omega t + j\frac{2\pi}{3} + \alpha\right) \\ &+0.5 I_m V_{mu}\cos\left(\omega t + \theta_u - \pi/2\right)\cos\left(\omega t + j\frac{2\pi}{3} + \alpha\right) + v_{dc} i_{dc}/6 - L_t \tilde{i}_{dcrip} i_{dc}/9 \\ &-R_t i_{dc}^2/9 + \frac{i_{dc}V_{mu}}{3}\cos\left(\omega t + \theta_u - \pi/2\right) \end{aligned} \tag{13}$$

After some simplifications, the final equation of the instantaneous power of the MMC upper sub-modules can be obtained as,

$$\begin{aligned} p_{uk} &= \beta_{u0} + \beta_{u11}\cos\left(\omega t + j\frac{2\pi}{3} + \alpha\right) + \beta_{u12}\cos\left(\omega t + \theta_u - \pi/2\right) + \beta_{u2}\cos\left(2\omega t + \theta_u + \alpha - \pi/2 + j\frac{2\pi}{3}\right) \\ \beta_{u0} &= v_{dc} i_{dc}/6 - L_t \tilde{i}_{dcrip} i_{dc}/9 - R_t i_{dc}^2/9 + 0.25 I_m V_{mu}\cos\left(j\frac{2\pi}{3} - \theta_u + \alpha + \pi/2\right) \\ \beta_{u11} &= 0.25 I_m v_{dc} - \frac{I_m L_t \tilde{i}_{dcrip}}{6} - \frac{i_{dc}R_t I_m}{6} \\ \beta_{u12} &= \frac{V_{mu} i_{dc}}{3} \\ \beta_{u2} &= 0.25 I_m V_{mu} \end{aligned} \tag{14}$$

The same calculations are performed for the power of the lower sub-modules, and consequently,

$$
\begin{aligned}
&p_{lk} = -i_{lk} v_{lk} = \\
&\beta_{l0} + \beta_{l11} \cos\left(\omega t + j\frac{2\pi}{3} + \alpha \right) + \beta_{l12} \cos\left(\omega t + \theta_l - \pi/2 \right) + \beta_{l2} \cos\left(2\omega t + \theta_l + \alpha - \pi/2 + j\frac{2\pi}{3} \right) \\
&\beta_{l0} = v_{dc} i_{dc} / 6 - R_t i_{dc}^2 / 9 - i_{dc} L_t \tilde{i}_{dcrip} / 9 - 0.25 I_m V_{ml} \cos\left(j\frac{2\pi}{3} - \theta_l + \alpha + \pi/2 \right) \\
&\beta_{l11} = -0.25 I_m v_{dc} + \frac{i_{dc} R_t I_m}{6} - \frac{L_t \tilde{i}_{dcrip} I_m}{6}, \quad \beta_{l12} = \frac{V_{ml} i_{dc}}{3}, \quad \beta_2 = -0.25 I_m V_{ml}
\end{aligned}
\tag{15}
$$

Where, β_i in equations (14) and (15) are the coefficients of the instantaneous dc power and harmonic components which can be changed by the MMC's specifications such as parameters like currents and voltages. According to (14) and (15), the instantaneous powers of the upper and lower sub-modules comprise two parts: dc component and harmonic components at the main and second-order frequency of the MMC operating condition.

4.2. Instantaneous Power of the Arm's Resistance and Inductance

Another part of the MMC arm is associated with the arm resistance and inductance. From Fig.1.a, the voltage of the upper arm resistance and inductance can be achieved as,

$$
v_{ux} = L_t \frac{di_{uk}}{dt} + R_t i_{uk} \tag{16}
$$

Substituting (4) in (16), the sum of the voltages of the upper arm resistance and inductance can be written as,

$$
v_{ux} = -0.5 I_m L_t \omega \sin\left(\omega t + j\frac{2\pi}{3} + \alpha \right) + L_t \tilde{i}_{dcrip} / 3 + 0.5 I_m R_t \cos\left(\omega t + j\frac{2\pi}{3} + \alpha \right) + i_{dc} R_t / 3 \tag{17}
$$

Thus, the power corresponding to this voltage can be obtained as,

$$
p_{ux} = i_{uk} v_{ux} \tag{18}
$$

Using (4) and (17), (18) can be rewritten as,

$$
\begin{aligned}
&p_{ux} = \beta_{xu0} + \beta_{xu11} \cos\left(\omega t + j\frac{2\pi}{3} + \alpha \right) + \beta_{xu12} \cos\left(\omega t + j\frac{2\pi}{3} + \alpha - \frac{\pi}{2} \right) \\
&+ \beta_{xu21} \cos\left(2\omega t + j\frac{4\pi}{3} + 2\alpha \right) + \beta_{xu22} \cos\left(2\omega t + j\frac{4\pi}{3} + 2\alpha - \frac{\pi}{2} \right) \\
&\beta_{xu0} = 0.125 I_m^2 R_t + \frac{L_t \tilde{i}_{dcrip} i_{dc}}{9} + \frac{i_{dc}^2 R_t}{9} \\
&\beta_{xu11} = \frac{I_m L_t \tilde{i}_{dcrip}}{6} + \frac{i_{dc} R_t I_m}{3}, \quad \beta_{xu12} = -\frac{I_m L_t i_{dc} \omega}{6} \\
&\beta_{xu21} = 0.125 I_m^2 R_t, \quad \beta_{xu22} = -0.125 \omega L_t I_m^2
\end{aligned}
\tag{19}
$$

Again, from Fig.1.a, the below relation can be written for the voltage of the lower arm resistance and inductance as,

$$v_{lx} = L_t \frac{di_{lk}}{dt} + R_t i_{lk} \tag{20}$$

Consequently, performing the same scenario for the lower arm resistance and inductance voltage and observing the power law, the instantaneous power of the lower arm resistance and inductance can be achieved as,

$$\begin{aligned} p_{lx} &= -i_{lk} v_{lx} = \beta_{xl0} + \beta_{xl11} \cos\left(\omega t + j\frac{2\pi}{3} + \alpha\right) + \beta_{xl12} \cos\left(\omega t + j\frac{2\pi}{3} + \alpha - \frac{\pi}{2}\right) \\ &+ \beta_{xl21} \cos\left(2\omega t + j\frac{4\pi}{3} + 2\alpha\right) + \beta_{xl22} \cos\left(2\omega t + j\frac{4\pi}{3} + 2\alpha - \frac{\pi}{2}\right) \\ \beta_{xl0} &= -0.125 I_m^2 R_t - \frac{L_t \tilde{i}_{dcrip} i_{dc}}{9} - \frac{i_{dc}^2 R_t}{9} \\ \beta_{xl11} &= \frac{I_m L_t \tilde{i}_{dcrip}}{6} + \frac{I_m i_{dc} R_t}{6} + \frac{I_m R_t i_{dc}}{6} \\ \beta_{xl12} &= -\frac{I_m L_t \omega i_{dc}}{6}, \beta_{xl21} = -0.125 I_m^2 R_t, \beta_{xl22} = 0.125 I_m^2 L_t \omega \end{aligned} \tag{21}$$

where β_{xu} and β_{xl} are the dc and ac component coefficients of the upper and lower arm resistance and inductance instantaneous power. These coefficients are completely dependent on the MMC parameters and its operating conditions at the output and input sides. Thus, accurate calculation of these powers is considerably dependent on the proper operation of the MMC in different conditions of the steady and dynamic states, which can be achieved by executing the appropriate control technique.

5. Determination of I_m and α

It can be understood from the proposed modulation functions of (10) and (11) that the main parts of these functions are completely relevant to the specifications of the MMC output currents. On the other hands, considering the obtained equation related to arm's instantaneous powers, it can be seen that the magnitude and angle phase of the MMC output currents have significant effects on all power components. Thus, for presenting an accurate control strategy, the calculation of the output of the MMC current specifications is done in this section based on its rated output active and reactive power. The instantaneous active and reactive power of the proposed MMC are written as,

$$p_{3\varphi} = 1.5 V_m I_m \cos(\alpha) \tag{22}$$

$$q_{3\varphi} = 1.5 V_m I_m \sin(\alpha) \tag{23}$$

Dividing (23) by (22) and using the achieved phase angle in (22), the main parts of the MMC output current can be obtained as (24),

$$I_m = \frac{p_{3\varphi}}{1.5V_m \cos\left(\tan^{-1}\left(\frac{q_{3\varphi}}{p_{3\varphi}}\right)\right)}, \qquad \alpha = \tan^{-1}\left(\frac{q_{3\varphi}}{p_{3\varphi}}\right) \tag{24}$$

For the proposed modulation-based control technique related to the MMC with specified output active and reactive power, (24) is employed to perform accurately the controlling operation of the MMC in different working states.

6. Accurate sizing of the equivalent sub-module capacitors

Considering the output operation of the MMC sub-modules, each sub-module has various output voltage during different operating conditions. Thus, the equivalent capacitor of sum of the upper or lower sub-modules is varied during the MMC performance along with the proposed controller. Taking into account, the upper and lower arm currents of the MMC, the size of the equivalent capacitor can be written as,

$$i_{uk} = C_{equ}\frac{dv_{uk}}{dt} \Rightarrow C_{equ} = \frac{i_{uk}}{\left(dv_{uk}/dt\right)} \tag{25}$$

$$i_{lk} = -C_{eql}\frac{dv_{lk}}{dt} \Rightarrow C_{eql} = \frac{-i_{lk}}{\left(dv_{lk}/dt\right)} \tag{26}$$

By substituting the obtained equations related to the upper and lower voltages and currents in (25) and (26), the equivalent capacitors of the upper and lower sub-modules respectively are derived as,

$$C_{equ} = \frac{0.5I_m \cos\left(\omega t + j\frac{2\pi}{3} + \alpha\right) + i_{dc}/3}{0.5\tilde{v}_{dc} - R_t\tilde{i}_{dcrip}/3 - V_{mu}\omega\sin\left(\omega t + \theta_u - \pi/2\right)} \tag{27}$$

$$C_{eql} = \frac{-0.5I_m \cos\left(\omega t + j\frac{2\pi}{3} + \alpha\right) + i_{dc}/3}{0.5\tilde{v}_{dc} - R_t\tilde{i}_{dcrip}/3 - V_{ml}\omega\sin\left(\omega t - \theta_l - \pi/2\right)} \tag{28}$$

Equations (27) and (28) are drawn in Fig.2. As it can be seen from these figures, both equivalent capacitors of upper and lower sub-modules are changed in operation state of MMC which can show the variable feature of arms capacitors. Suitable operation of MMC can lead to accurate calculation of these capacitors.

7. Simulation results

Matlab/Simulink environment in discrete mode is employed to evaluate the validity of the proposed modulation function-based control technique under various operating conditions. The overall structure of the proposed controller is drawn in Fig. 3. As it can be seen from this figure,

two processes of the MMC load and parameters changes are applied to the proposed MMC in inverter mode, which shall be further discussed in this section. The values of these processes are given in Table II. Moreover, to fulfil acceptable simulation results, the sample time of the simulation is considered in 1 micro seconds (μs). In both processes, ac capacitor filter is utilized at the PCC, the value of which is presented in Tables 1 and 2.

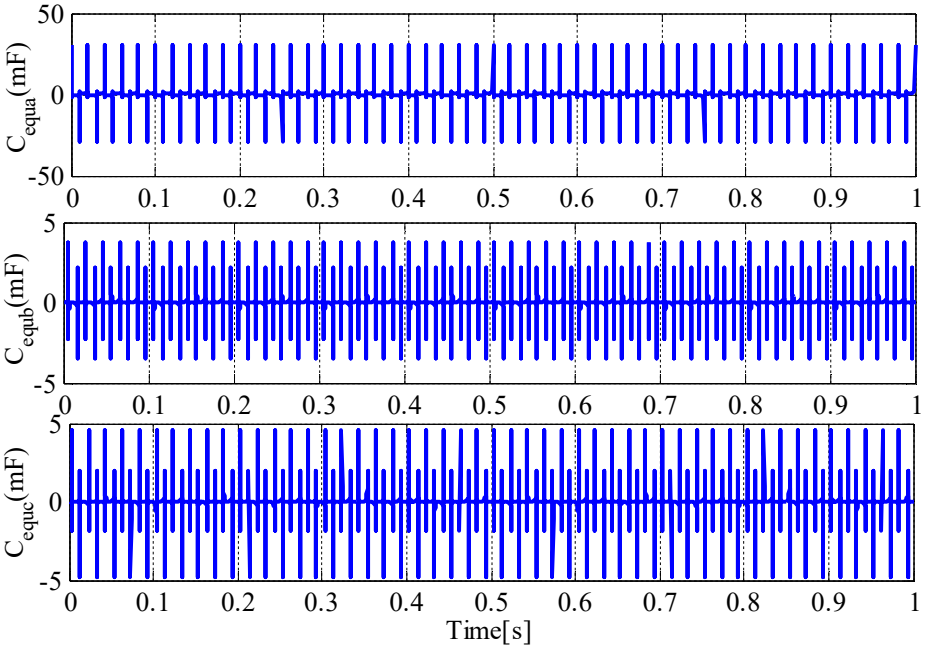

(a)

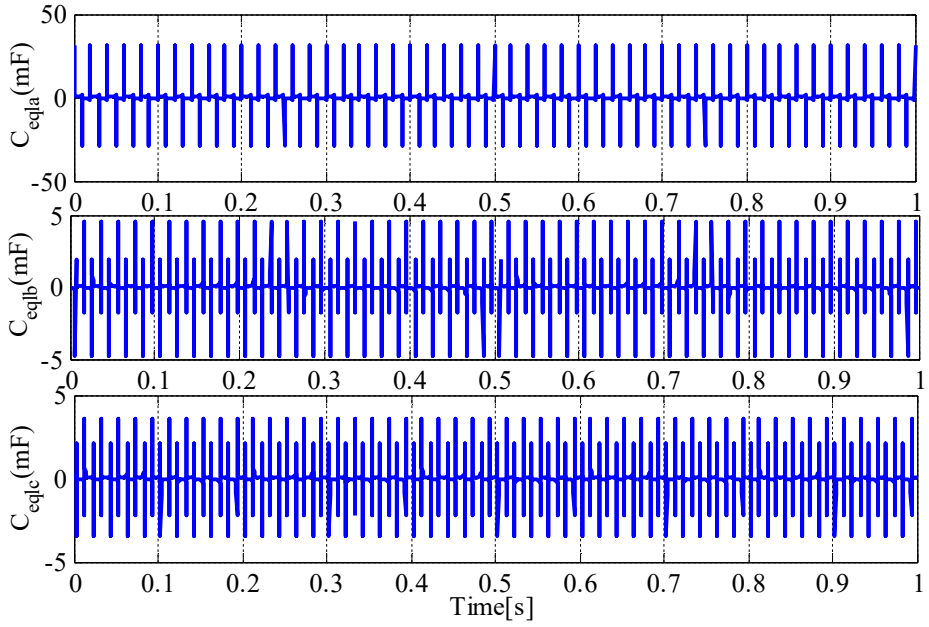

(b)

Fig. 2*. The equivalent capacitor of (a) upper sub-modules (b) lower sub-modules.*

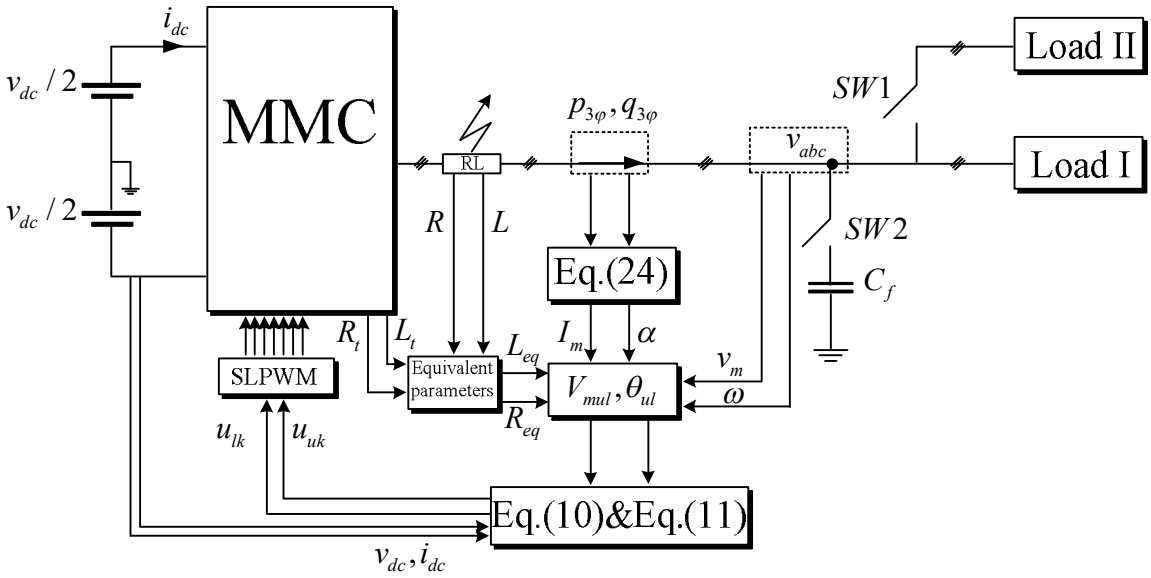

***Fig. 3**. The overall structure of the proposed controller.*

Table 1: The parameters of the proposed MMC in load changes conditions

Parameters	Value	Parameters	Value
$L_t(mH)$	15	N	4
$L(mH)$	6	$f(Hz)$	50
$R_t(\Omega)$	0.6	Load Active Power I	50 kW
$R(\Omega)$	0.1	Load Reactive Power I	20 kVAR
$v_{dc}(V)$	11200	Load Active Power II	35 kW
$v_m(V)$	5800	Load Reactive Power II	25 kVAR

Table 2: The parameters of the proposed MMC in parameters changes conditions

Parameters	Value	Parameters	Value
$L_{t1}(mH)$	15	$R_2(\Omega)$	0.15
$L_1(mH)$	6	$v_{dc}(V)$	11200
$R_{t1}(\Omega)$	0.6	$v_m(V)$	5800
$R_1(\Omega)$	0.1	N	4
L_{t2}(mH)	25	*f(Hz)*	50
L_2(mH)	9	Load Active Power	50 kW
$R_{t2}(\Omega)$	0.9	Load Reactive Power	20 kVAR

7.1. Load Changes Evaluation

Firstly, the proposed MMC is set to supply the load of 50 kW and 20 kVAR in the time duration of [0 s, 0.2 s] that is considered as steady-state period. Then, at t=0.2 s, a load of 35 kW and 25 kVAR will be connected to the PCC and the MMC is responsible for the generation of the needed power to cope with additional load. For the specified active and reactive power of the MMC, the variables I_m and α will be calculated from (24) to be used in the proposed modulation function. The MMC parameters in this section are given in Table II. The proposed upper and lower modulation functions of the MMC-based control technique with its carrier waves during load dynamic change are illustrated in Fig.4.a. The changes created in these functions at t=0.2s are used to make a proper control performance for generating the needed switching signals of the MMC sub-modules. Figs.4.b and c show the generated switching signals for sub-modules of phase "a". It can be realized from these figures that there is an inverse pattern for upper and lower sub-modules so that the needed switching signals are generated through SLPWM shown in Fig.4.a for reaching the control aims under load change.

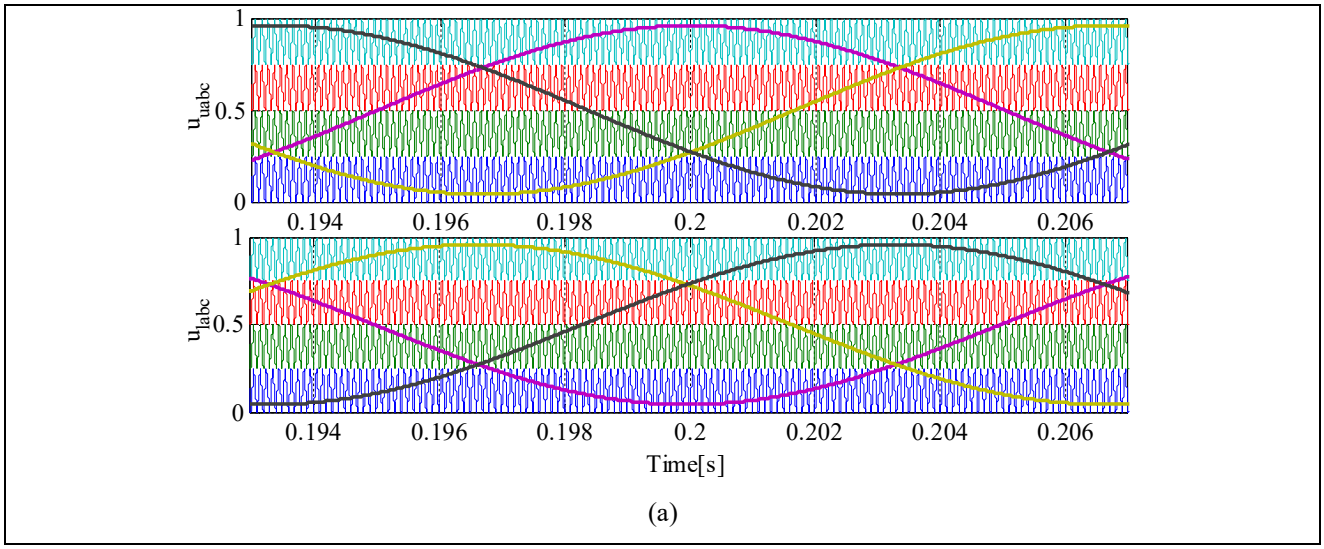

(a)

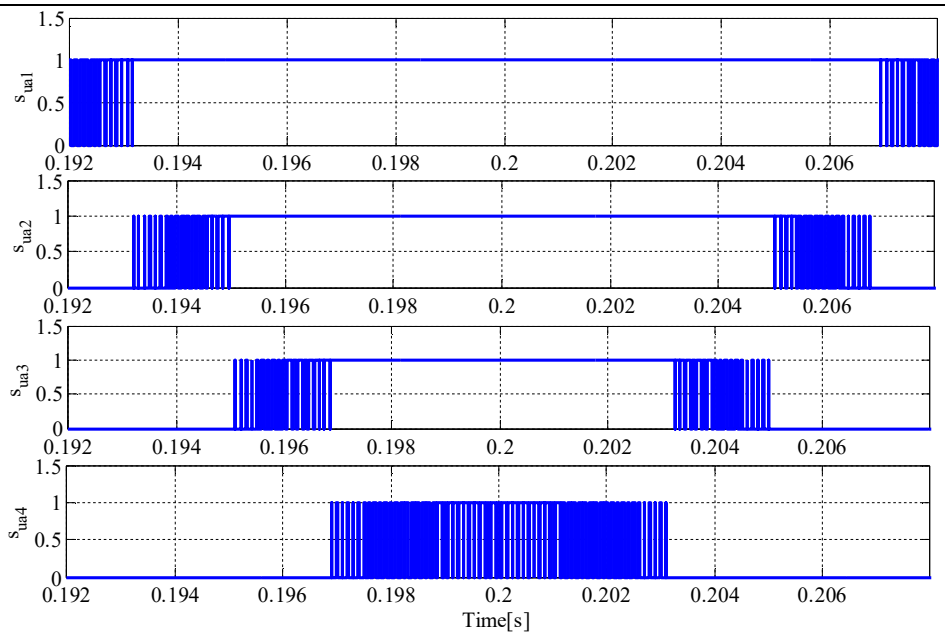

(b)

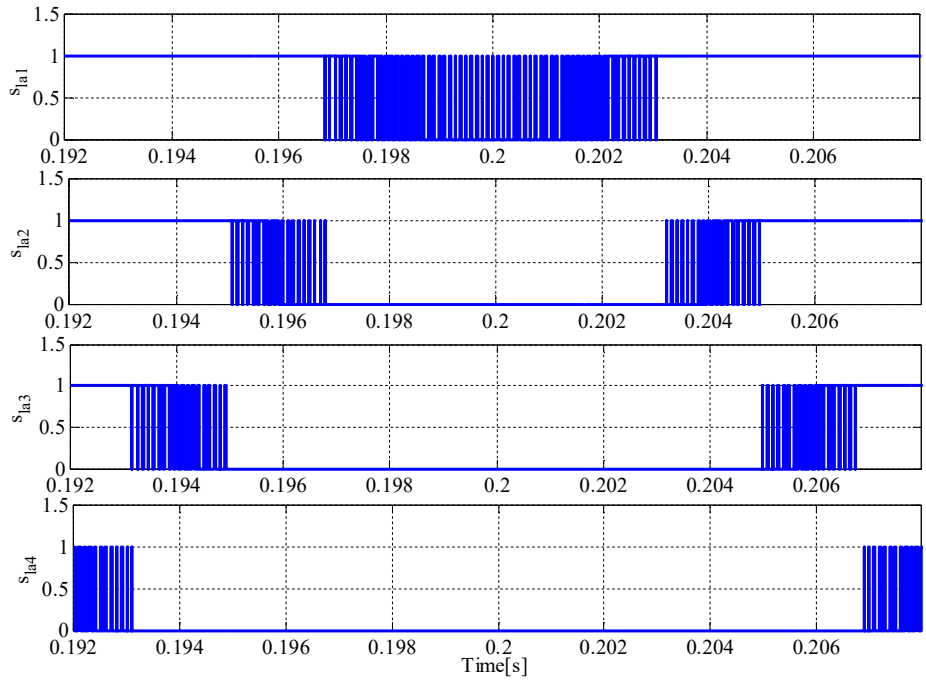

(c)

Fig. 4. *In load changes process, a) The proposed three-phase upper and lower modulation functions with its carrier waves, b)the generated switching signals for upper sub-modules in phase "a" c) the generated switching signals for lower sub-modules in phase "a"*

The performance of the proposed controller at the desired control of the sub-modules voltages is shown in Fig. 5.a. According to this figure, the sub-module voltages in steady state are kept within the desired value region of 2.8 kV. After load dynamic change, the desired value of the sub-module voltages can be properly achieved with negligible transient response which proves the proper dynamic operation of the proposed controller. The output ac voltages of the MMC before

and after using ac filter capacitor ($C_f = 50\mu F$) are shown in Fig.5.b, which validates the accurate performance of the designed modulation-based controller in both operating conditions.

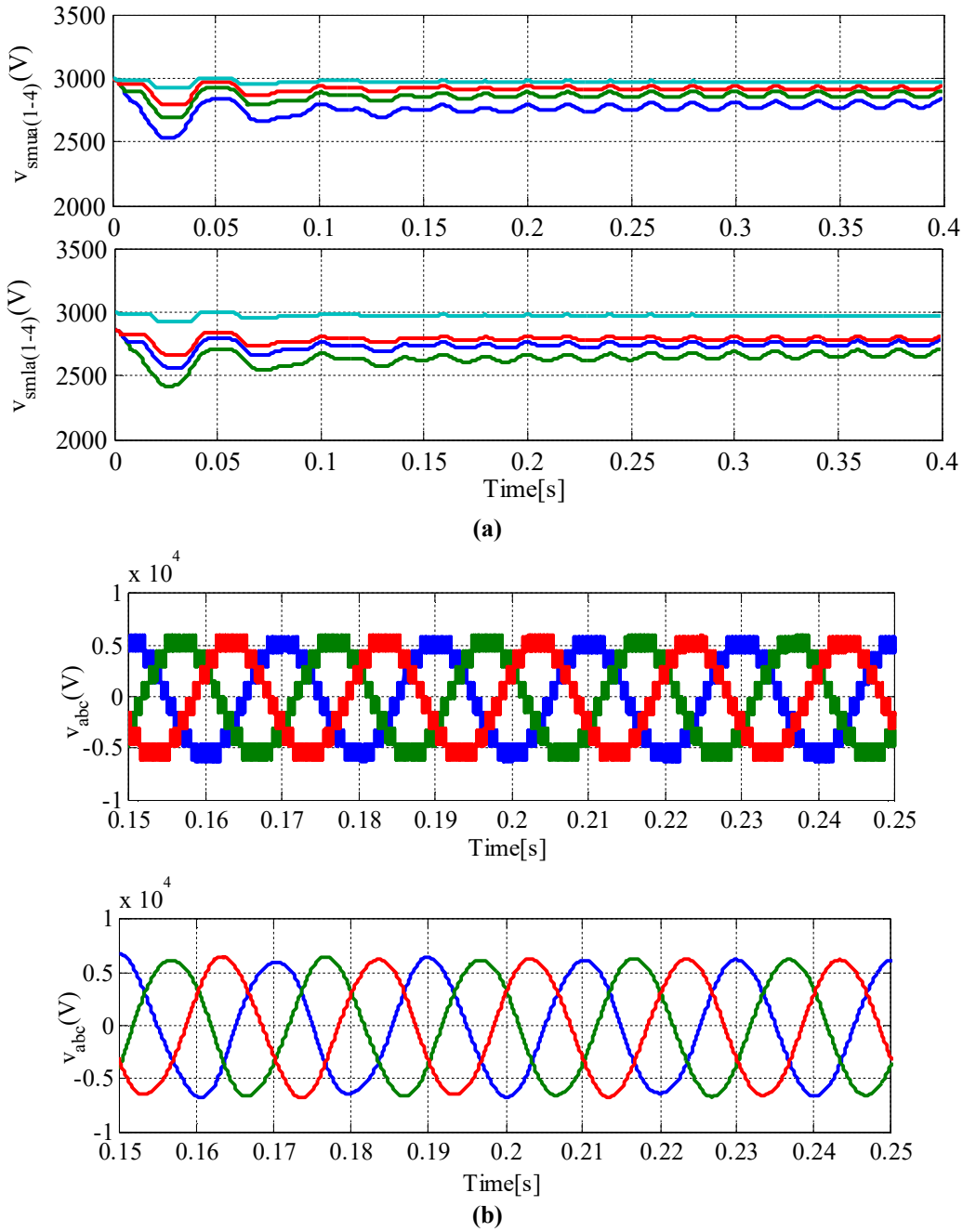

Fig. 5*. (a) The sub-module voltages of phase "a" (b) The output voltages of MMC before and after connecting ac filter capacitor under load change condition*

The output and circulating currents assessment of the MMC is accomplished in Fig.6.a. This figure verifies the capability of the MMC at generating suitable output currents in both steady state and dynamic operating conditions. Moreover, as can be seen, the MMC's circulating currents almost tend to be zero with the slight fluctuations.

The capability of MMC for active and reactive power sharing is indicated in Fig. 6.b. According to this figure, the MMC's active power properly follows the total load active power in

both operating conditions. Fig. 6.b demonstrates the ability of the proposed controller at tracking the reactive power of load in both conditions. Fig.7 shows the angle difference between output MMC voltages and Currents under load changes condition. As it can be seen in Fig.7, this angle is appropriately changed according to the MMC active and reactive power needed for load.

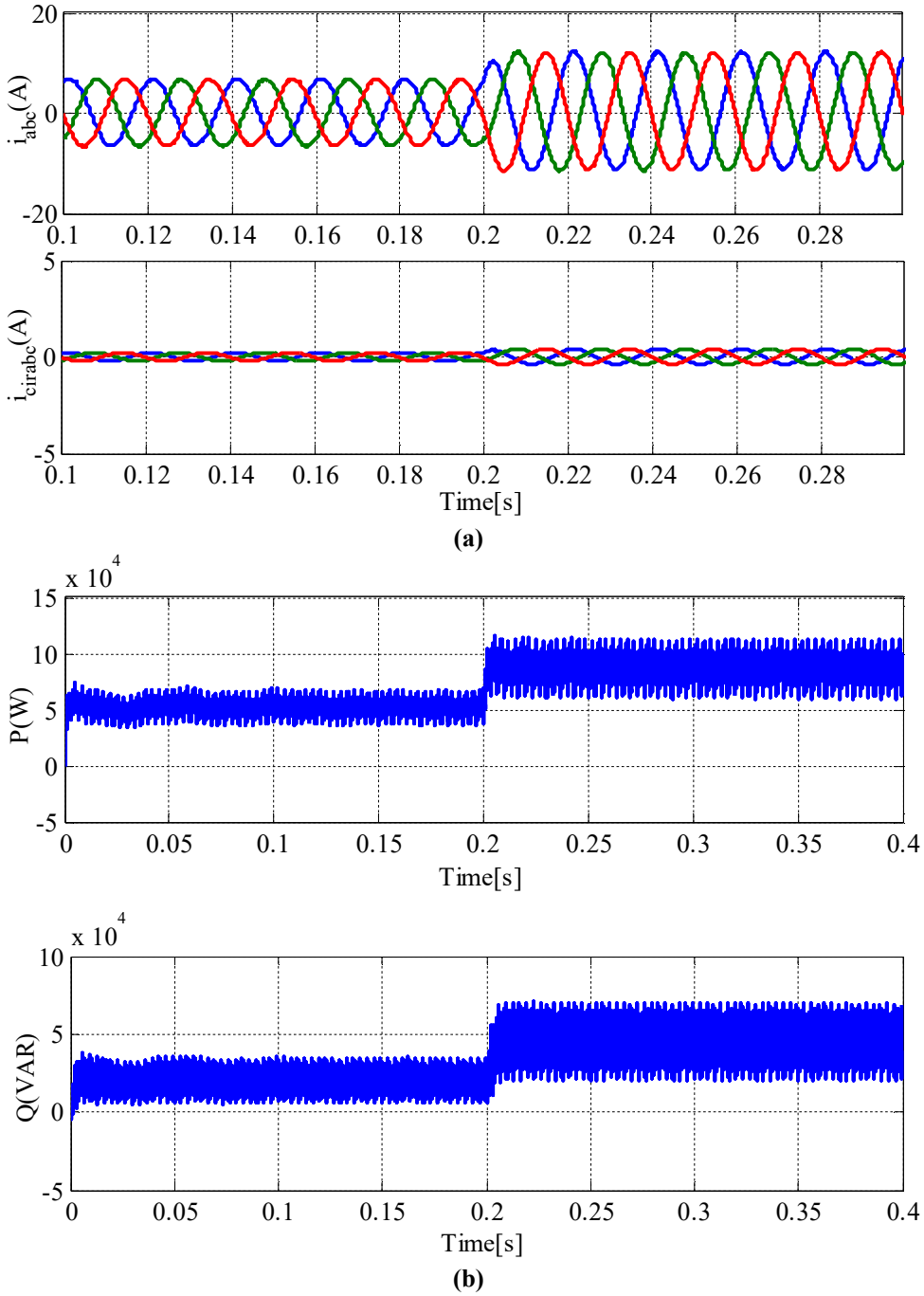

Fig. 6*. (a) The output and circulating currents of the MMC. (b) Active and reactive power of the MMC under load changes condition.*

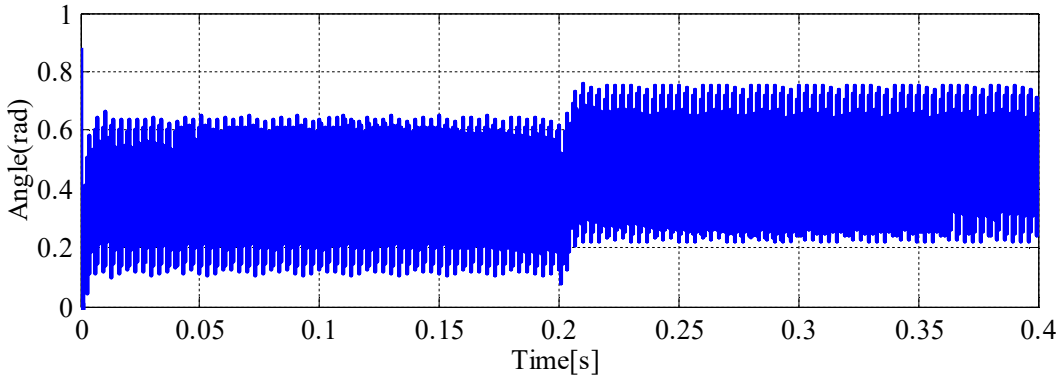

***Fig.** 7. Angle Difference between output MMC voltages and Currents under load changes condition.*

7.2. Parameters Changes Evaluation

In this section, the effects of varying the MMC parameters on the proposed modulation-based control technique are investigated. Two collections of the parameters corresponding to the MMC's resistances and inductances are given in Table II, which presents the MMC parameters in two different operation conditions. The MMC parameters are varied to the second condition in t=0.2 s. In this process, the MMC supplies a constant load of 50 kW and 20 kVAR. In the presence of the parameters alterations, the proposed modulation functions varied as depicted in Fig.8.a. The related carrier waves are also given in Fig.8.a. The changes made in the functions leads to a different trend for the applied PWM, upon which the appropriate control operation will be finally executed for the proposed MMC. By using SLPWM presented in Fig.8.a, the switching signals for upper and lower sub-modules of phase "a" are achieved illustrated in Fig.8.b and c, respectively. The same pattern is governed in this section. However, the control aim is following the reference values under MMC parameters changes in which switching signals are adapted according this aim.

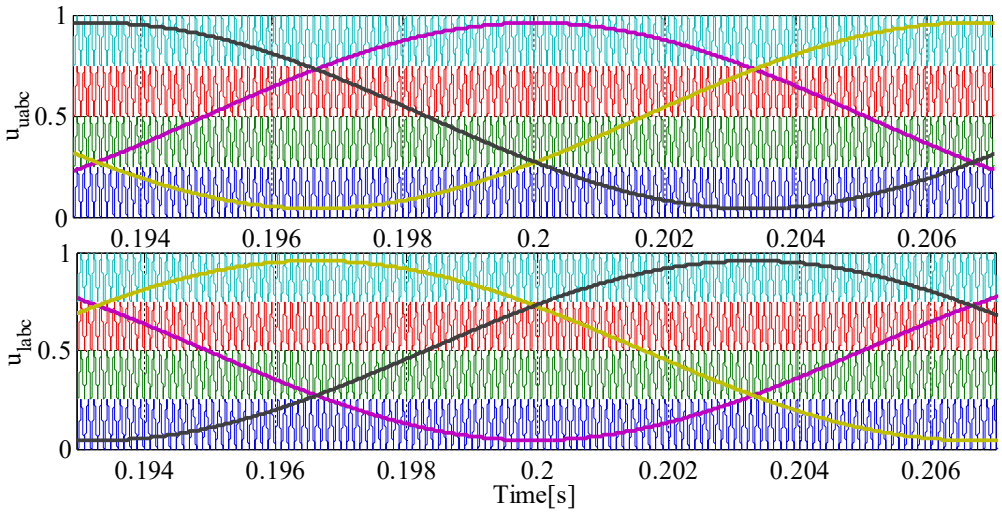

(a)

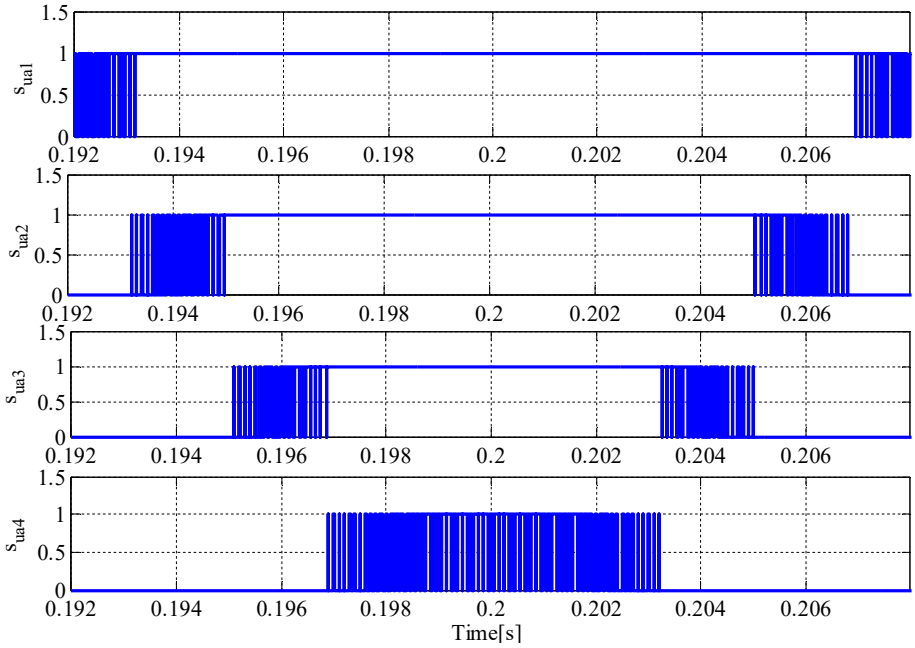

(b)

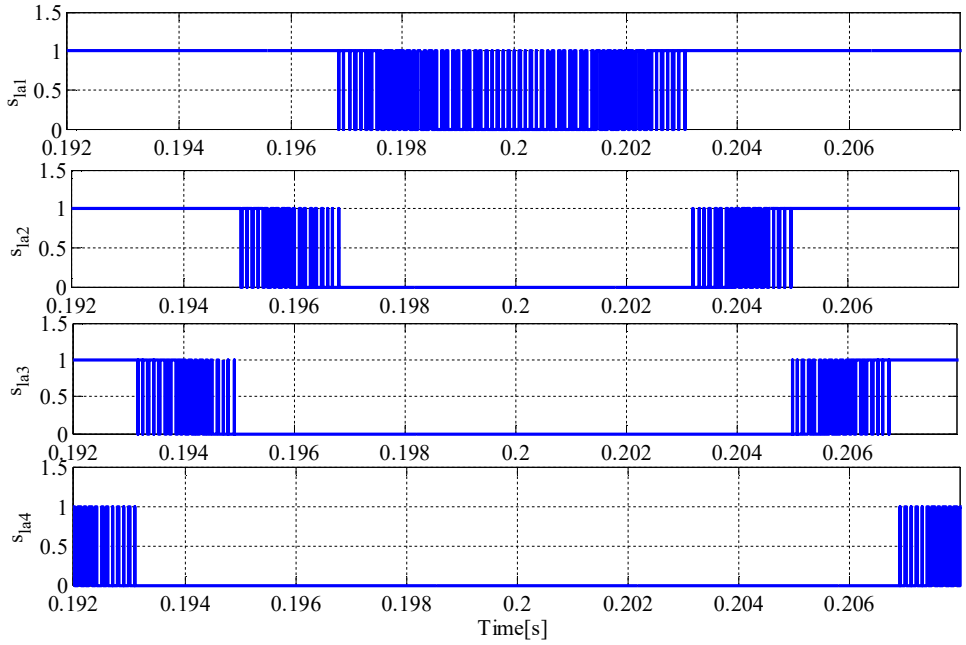

(c)

Fig. 8. *In parameters changes condition, a) The proposed three-phase upper and lower modulation functions with its carrier waves, b)the generated switching signals for upper sub-modules in phase "a" c) the generated switching signals for lower sub-modules in phase "a"*

The first aim of the proposed controller is to regulate the sub-module voltages. As it can be seen in Fig.9.a, after varying the parameters at t=0.2s, the proposed controller is able to maintain the sub-module voltages around the desired value regardless of the small fluctuations in short transient time. The output voltages of MMC during ac filter capacitor ($C_f = 50\mu F$) connection and disconnection are shown in Fig. 9.b. The proposed controller is able to keep these voltages at its desired values in parameters changes condition as shown in Fig. 9.b.

The output and circulating currents of MMC are shown in Fig.10.a. According to this figure, the sinusoidal output current is proportional to the consumed load. Also, it is realized form Fig.10.a that the proposed controller is able to reach the desired value of the output currents with the existence of MMC parameters variations. Moreover, it can be observed from Fig.10.a that the operation of the proposed controller in both steady and dynamic state for minimizing the circulating current is good. The active and reactive powers of the MMC are displayed in Fig. 10.b. According to this figure, the MMC parameters variation have no significant effects on the active and reactive power sharing of the MMC, as the MMC properly generates the required active power of the load. Fig.11 shows the angle difference between output MMC voltages and Currents under MMC parameters changes condition. It can be understood from Fig.11 that the angle values are kept in limited area with suitable instantaneous alterations leading to constant active and reactive power in presence of MMC parameters changes.

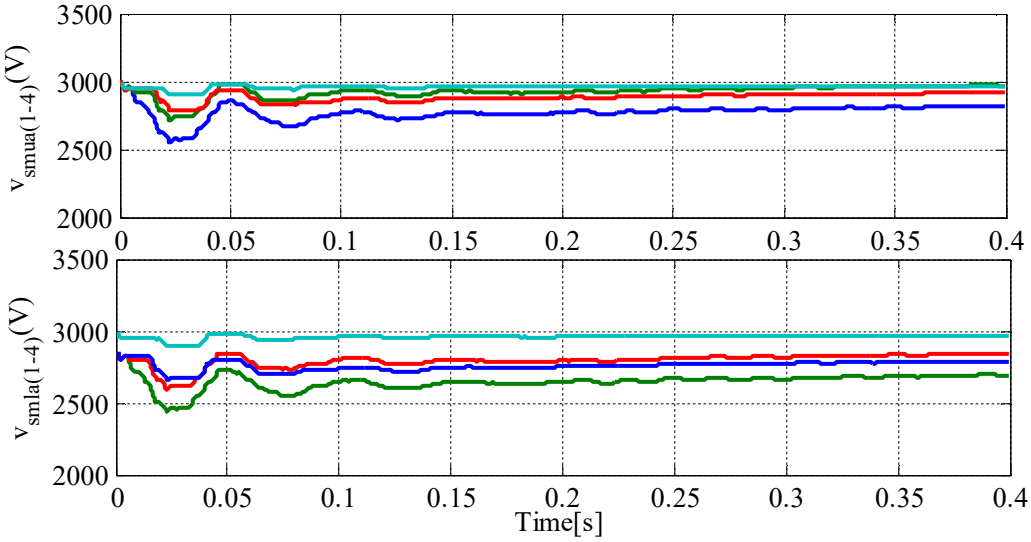

(a)

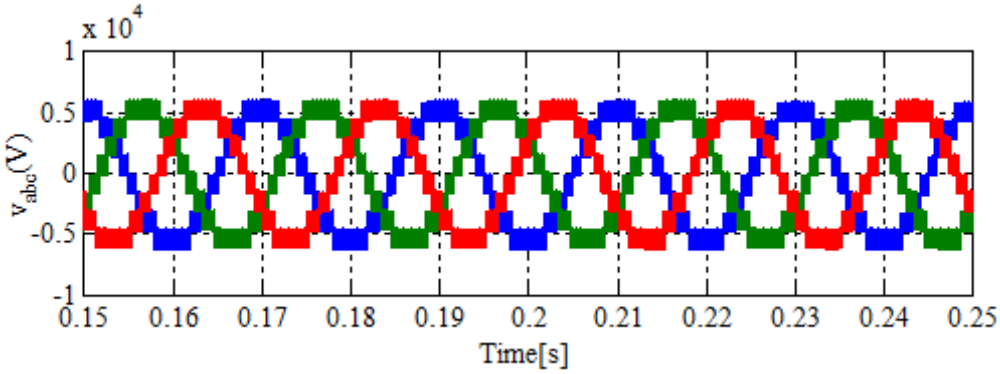

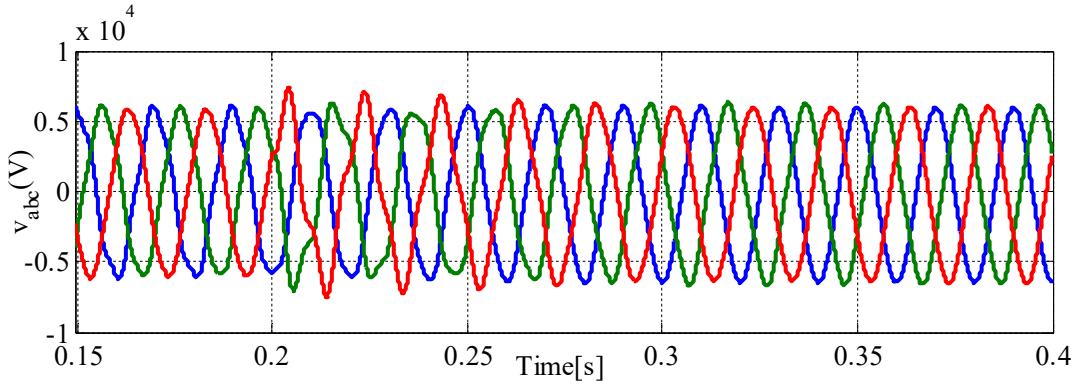

(b)

Fig. 9*. (a)The sub-modules voltages of phase "a" (b) Output voltages of MMC before and after connecting ac filter under parameters change condition.*

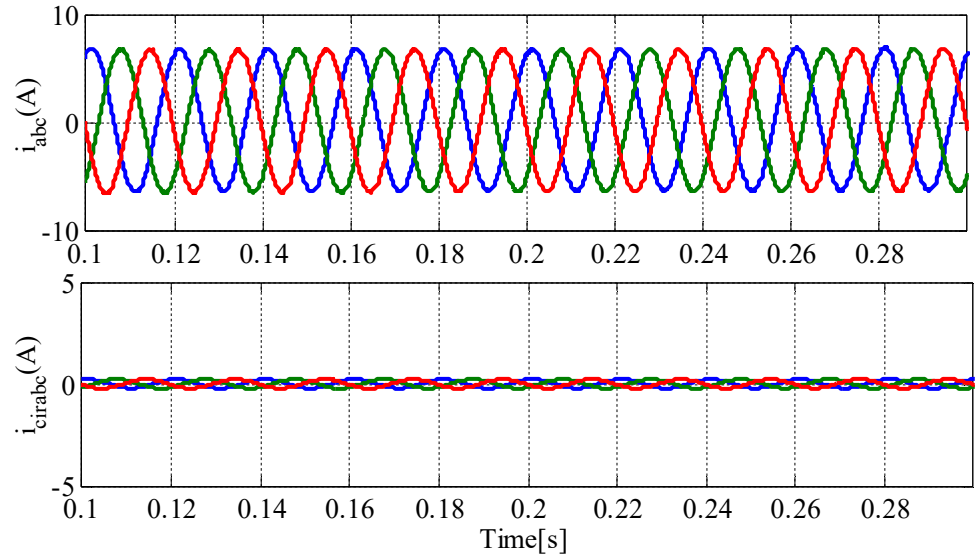

(a)

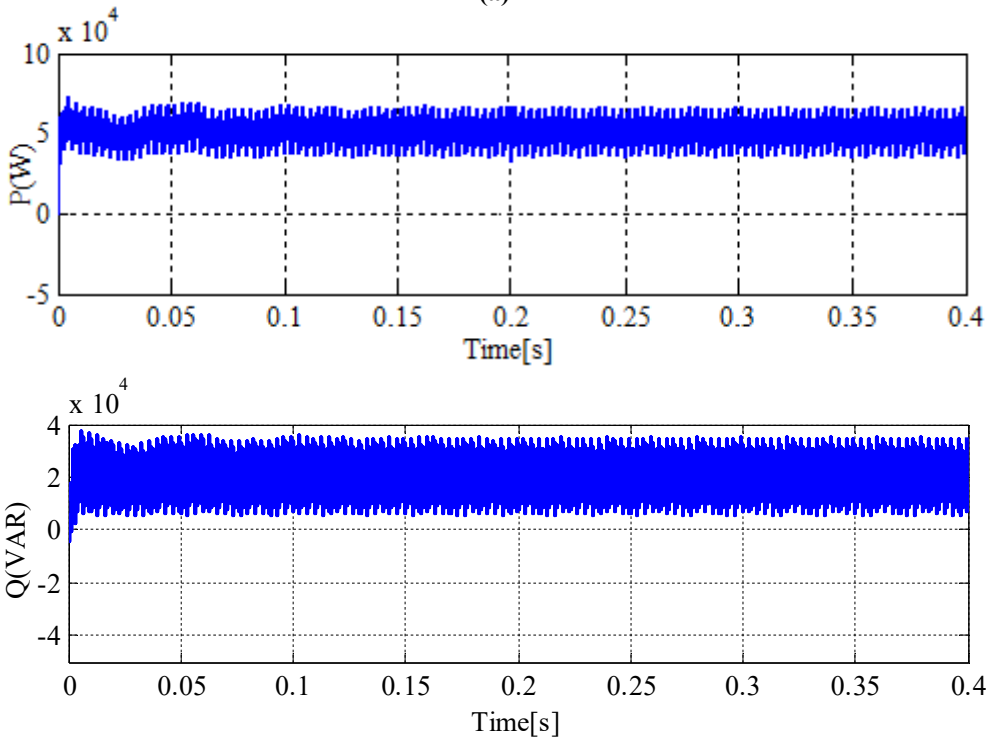

(b)

Fig. 10. *(a) Output and circulating currents of the MMC (b) Active and reactive power of the MMC under parameters changes condition*

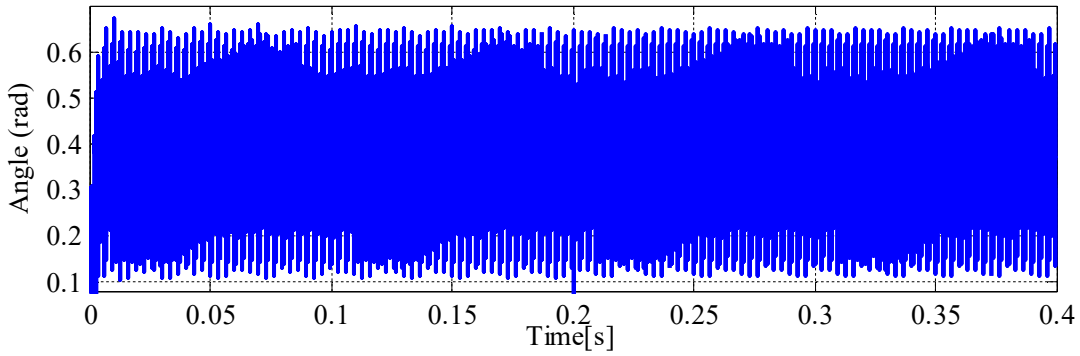

***Fig. 11**. Angle Difference between output MMC voltages and Currents under parameters changes condition*

8. Conclusion

The main contributions of this paper are two separate modulation functions proposed for the generation of the switching signals of the MMC upper and lower sub-modules. The MMC arms currents, driven from circulating and output currents are applied to the mathematical model of the converter in *a-b-c* reference frame. This proposed modulation functions are simple in construction when compared with other control methods. It also stabilized the operation of the system in periods of parameters varying conditions. Changing the load connected to the PCC and MMC parameters was considered for the assessment of the designed controller, which was responsible for the control of the sub-modules voltages and accurate active and reactive power sharing performance. To complete the evaluation of the proposed controller, the instantaneous power of the MMC arms and the equivalent capacitors of the sub-modules were investigated. The simulation results in Matlab/Simulink environment demonstrated the capability of the proposed controller at reaching the main control purposes.

9. Acknowledgments

This work was supported by FEDER funds through COMPETE 2020 and by Portuguese funds through FCT, under Projects SAICT-PAC/0004/2015 - POCI-01-0145-FEDER-016434, POCI-01-0145-FEDER-006961, UID/EEA/50014/2013, UID/CEC/50021/2013, UID/EMS/00151/2013 and SFRH/BPD/102744/2014. Also, the research leading to these results has received funding from the EU Seventh Framework Programme FP7/2007-2013 under grant agreement no. 309048.

10. Appendix

$$V_{mu}=\sqrt{\left[I_m R_{eq}\sin(\alpha)+L_{eq}I_m\omega\cos(\alpha)\right]^2+\left[L_{eq}I_m\omega\sin(\alpha)-I_m R_{eq}\cos(\alpha)+v_m\right]^2},\ \theta_u=tag^{-1}\left(\frac{\left[L_{eq}I_m\omega\sin(\alpha)-I_m R_{eq}\cos(\alpha)+v_m\right]}{\left[I_m R_{eq}\sin(\alpha)+L_{eq}I_m\omega\cos(\alpha)\right]}\right)$$

$$V_{ml}=\sqrt{\left[I_m R_{eq}\sin(\alpha)+L_{eq}I_m\omega\cos(\alpha)\right]^2+\left[-v_m-R_{eq}I_m\cos(\alpha)+L_{eq}I_m\omega\sin(\alpha)\right]^2},\theta_l=tag^{-1}\left(\frac{\left[-v_m-R_{eq}I_m\cos(\alpha)+L_{eq}I_m\omega\sin(\alpha)\right]}{\left[L_{eq}I_m\omega\cos(\alpha)+R_{eq}I_m\sin(\alpha)\right]}\right)$$

11. References

[1] Wang, C., Ooi B-T.: 'Incorporating deadbeat and low-frequency harmonic elimination in modular multilevel converters', IET Generation, Transmission & Distribution., 2015, 9, (4), pp. 369 – 378.

[2] Pouresmaeil, E., Mehrasa, M., Shokridehaki, MA., Rodrigues, E., Catalao, JPS.: ' Control of Multi Modular Converters for Integration of Distributed Generation Sources into the Power Grid', in Proc. IEEE International Conference on Smart Energy Grid Engineering (SEGE)., 2015, pp. 1-6.

[3] Mei, J., Xiao, B., Shen, K., Tolbert, LM., Zheng, JY.: 'Modular Multilevel Inverter with New Modulation Method and Its Application to Photovoltaic Grid-Connected Generator', IEEE Trans. Power Electron., 2013, 28, (11), pp. 5063 - 5073.

[4] Tu, Q., Xu, Z., Xu, L.: 'Reduced Switching-Frequency Modulation and Circulating Current Suppression for Modular Multilevel Converters', IEEE Trans. Power Delivery, 2011, 26, (3), pp. 2009 - 2017.

[5] Harnefors, L., Antonopoulos, A., Norrg, S., Ängquist, L., Nee, HP.: 'Dynamic Analysis of Modular Multilevel Converters', IEEE Trans. Industrial Electronic., 2013, 60, (7), pp. 2526 - 2537.

[6] Vasiladiotis, M., Cherix, N., Rufer, A.: 'Accurate Capacitor Voltage Ripple Estimation and Current Control Considerations for Grid-Connected Modular Multilevel Converters' , IEEE Trans. Power Electronic., 2014, 29, (9), pp. 4568 - 4579.

[7] Liu, S., Xu, Z., Hua, W., Tang, G., Xue, Y.: 'Electromechanical Transient Modeling of Modular Multilevel Converter Based Multi-Terminal HVDC Systems', IEEE Trans. Power System., 2014, 29, (1), pp. 72 - 83.

[8] Chen, B., Chen, Y., Tian, C., Yuan, J., Yao, X.: 'Analysis and Suppression of Circulating Harmonic Currents in a Modular Multilevel Converter Considering the Impact of Dead Time', IEEE Trans. Power Electronic., 2015, 30, (7), pp. 3542 - 3552.

[9] Fehr, H., Gensior, A., Muller, M.: 'Analysis and trajectory tracking control of a modular multilevel converter', IEEE Trans. Power Electronic., 2015, 30, (1), pp. 398 - 407.

[10] Perez, MA., Lizana, R., Arancibia, D., Espinoza, JR., Rodriguez, J.: 'Decoupled Currents Model and Control of Modular Multilevel Converters', IEEE Trans. Industrial Electronic., 2015, 62, (9), pp. 5382 - 5392.

[11] Qin, J., Saeedifard, M.: 'Predictive Control of a Modular Multilevel Converter for a Back-to-Back HVDC System', IEEE Trans. Power Delivery., 2012, 27, (3), pp. 1538 - 1547.

[12] Wang, W., Beddard, A., Barnes, M., Marjanovic, O.: 'Analysis of Active Power Control for VSC–HVDC', IEEE Trans. Power Delivery., 2014, 29, (4), pp. 1978 - 1988.

[13] Wang, C., Hao, Q., Ooi, B-T.: 'Reduction of low-frequency harmonics in modular multilevel converters (MMCs) by harmonic function analysis', IET Generation, Transmission & Distribution., 2014, 8, (2), pp. 328 – 338.

[14] Guruambeth, R., Ramabadran, R.: 'Fuzzy logic controller for partial shaded photovoltaic array fed modular multilevel converter', IET Power Electronics., 2016, 9, (8), pp. 1694 – 1702.

[15] Hu, P., Jiang, D., Zhou, Y., Liang, Y., Guo, J., Lin, Z.: 'Energy-balancing Control Strategy for Modular Multilevel Converters Under Sub-module Fault Conditions', IEEE Trans. Power Electronic., 2014, 29, (9), pp. 5021-5030.

[16] Li, B., Yang, R., Xu, D., Wang, G., Wang, W., Xu, D.: 'Analysis of the Phase-Shifted Carrier Modulation for Modular Multilevel Converters', IEEE Trans. Power Electronic., 2015, 30, (1), pp. 297-310.

[17] Zhang, Y., Adam, GP., Lim, TC., Finney, SJ., Williams BW.: 'Analysis of modular multilevel converter capacitor voltage balancing based on phase voltage redundant states', IET Power Electronics., 2012, 5, (6), pp. 726 – 738.

[18] Saeedifard, M., Iravani, R.: 'Dynamic Performance of a Modular Multilevel Back-to-Back HVDC System', IEEE Trans. Power Delivery., 25, (4), pp. 2903 - 2912.

[19] Deng, F., Chen, Z.: 'Voltage-Balancing Method for Modular Multilevel Converters Under Phase-Shifted Carrier-Based Pulse-Width Modulation', IEEE Trans. Industrial Electronic., 2015, 62, (7), pp. 4158 - 4169.

[20] Li, Z., Wang, P., Zhu, H., Chu, Z., Li, Y.: 'An Improved Pulse Width Modulation Method for Chopper-Cell-Based Modular Multilevel Converters', IEEE Trans. Power Electronic., 2012, 27, (8), pp. 3472 - 3481.

[21] Hu, P., Jiang, D.: 'A Level-Increased Nearest Level Modulation Method for Modular Multilevel Converters', IEEE Trans. Power Electronic., 2015, 30, (4), pp. 1836 - 1842.

[22] Picas, R., Ceballos, S., Pou, J., Zaragoza, J., Konstantinou, G., Agelidis, VG.: 'Closed Loop Discontinuous Modulation Technique for Capacitor Voltage Ripples and Switching Losses Reduction in Modular Multilevel Converters', IEEE Trans. Power Electronic., 2015, 30, (9), pp. 4714 - 4725.

[23] Fan, S., Zhang, K., Xiong, J., Xue, Y.: 'An Improved Control System for Modular Multilevel Converters with New Modulation Strategy and Voltage Balancing Control', IEEE Trans. Power Electronic., 2015, 30, (1), pp. 358 - 371.

[24] Hassanpoor, A., Ilves, K., Norrga, S., Ängquist, L., Nee, HP.: 'Tolerance Band Modulation Methods for Modular Multilevel Converters',15th European Conference on Power Electronics and Applications (EPE), 2013, pp. 1 - 10.

[25] Konstantinou, G., Ciobotaru, M., Agelidis, V.: 'Selective harmonic elimination pulse-width modulation of modular multilevel converters', IET. Power Electron., 2013, 6, (1), pp. 96–107.

[26] Siemaszko, D., Antonopoulos, A., Ilves, K., Vasiladiotis, M., Ängquist, L., Nee, HP., 'Evaluation of Control and Modulation Methods for Modular Multilevel Converters', The International Power Electronics Conference., 2010, pp. 746 - 753.

[27] Konstantinou, GS., Ciobotaru, M., Agelidis, VG.: 'Analysis of Multi-carrier PWM Methods for Back-to-back HVDC Systems based on Modular Multilevel Converters', 37th Annual Conference on IEEE Industrial Electronics Society., 2011, pp. 4391 - 4396.